







Metformin Hydrochloride Loaded Mucoadhesive Microspheres and Nanoparticles for Anti-Hyperglycemic and Anticancer Effects Using Factorial Experimental Design

Amina Alam Kotha ^{1,*}, Shihab Uddin Ahmad ^{2,3,*}, Irin Dewan ², Mohiuddin Ahmed Bhuiyan ², Fahad Imtiaz Rahman ¹, Isa Naina Mohamed ³, Md Selim Reza ¹

¹Department of Pharmaceutical Technology, Faculty of Pharmacy, University of Dhaka, Dhaka, 1000, Bangladesh; ²Department of Pharmacy, School of Medicine, University of Asia Pacific, Dhaka, 1215, Bangladesh; ³Department of Pharmacology, Faculty of Medicine, Universiti Kebangsaan Malaysia, Kuala Lumpur, 56000, Malaysia

*These authors contributed equally to this work

Correspondence: Md Selim Reza, Department of Pharmaceutical Technology, Faculty of Pharmacy, University of Dhaka, Dhaka, 1000, Bangladesh, Email selimreza@du.ac.bd; Isa Naina Mohamed, Department of Pharmacology, Faculty of Medicine, Universiti Kebangsaan Malaysia, Jalan Yaacob Latif, Bandar Tun Razak, Cheras, Kuala Lumpur, 56000, Malaysia, Email isanaina@ppukm.ukm.edu.my

Background: Metformin hydrochloride (HCl) microspheres and nanoparticles were formulated to enhance bioavailability and minimize side effects through sustained action and optimized drug-release characteristics. Initially, the same formulation design with different ratios of metformin HCl and Eudragit RSPO was used to formulate four batches of microspheres and nanoparticles using solvent evaporation and nanoprecipitation methods, respectively.

Methods: The produced formulations were evaluated based on particle size and shape (particle size distribution (PSD), scanning electron microscope (SEM)), incompatibility (differential scanning calorimetry (DSC), Fourier-transform infrared (FTIR)), drug release pattern, permeation behavior, in vivo hypoglycemic effects, and in vitro anticancer potential.

Results: Compatibility studies concluded that there was minimal interaction between metformin HCl and the polymer, whereas SEM images revealed smoother, more spherical nanoparticles than microspheres. Drug release from the formulations was primarily controlled by the non-Fickian diffusion process, except for A1 and A4 by Fickian, and B3 by Super case II. Korsmeyer-Peppas was the best-fit model for the maximum formulations. The best formulations of microspheres and nanoparticles, based on greater drug release, drug entrapment, and compatibility characteristics, were attributed to the study of drug permeation by non-everted intestinal sacs, in vivo anti-hyperglycemic activity, and in vitro anticancer activity.

Conclusion: This study suggests that the proposed metformin HCl formulation can dramatically reduce hyperglycemic conditions and may also have anticancer potential.

Keywords: microsphere, nanoparticles, permeability, anti-hyperglycemic, anticancer

Introduction

Diabetes mellitus (DM) is a widespread health concern and significant contributor to morbidity and mortality.¹⁻³ The WHO predicts that 80% of these deaths will occur in low- and middle-income countries and that these deaths will double between 2016 and 2030. Further estimates indicate that by 2030, there will be 438 million people worldwide with type-2 diabetes, up from 285 million in 2010. This unexpected increase is mostly due to genetic predispositions and variables associated with modern lifestyles such as stress, obesity, physical inactivity, and aging.⁴ Disruption of insulin production is a major factor in the development of DM and its associated issues, such as neuropathy, blindness, renal dysfunction, organ damage, and heart disease. The mortality rate of DM is 2–4 times greater than that of related diseases. The long-term management of type II

diabetes presents many challenges owing to the progressive nature and complexity of the disease. Multiple medications are typically required to achieve better glycemic control.^{5,6}

Metformin hydrochloride (HCl), a biguanide derivative, is the most common therapy for type-2 diabetes.^{7,8} It exerts its anti-hyperglycemic effect by reducing hepatic glucose production, limiting glucose absorption in the small intestine, enhancing insulin sensitivity in peripheral organs, suppressing gluconeogenesis, and lowering plasma free fatty acid.^{9–11} In addition, metformin has recently been discovered to be a potential cure for many cancers, particularly colon, prostate, and breast.¹²

Metformin is mostly absorbed through the upper small intestine after oral administration; however, its bioavailability is relatively poor. Its partial absorption can be improved by utilizing gastro-retentive drug delivery systems.^{7,13–16} In comparison to traditional dosage forms, metformin HCl particulate drug delivery methods, such as microspheres or nanoparticles, have several advantages, including higher local drug concentrations, reduced gastrointestinal transit time variability, low individual variability, low risk of dose dumping, reduced side effects, the ability to administer drugs via various routes (eg, parenteral, inhalation), and the ability to load hydrophilic and hydrophobic drugs.^{17–19} Additionally, metformin has attracted interest over the past two decades as a novel strategy for the treatment of cancer and has been applied in particle dosage forms, particularly in nano-particulate novel drug delivery systems, especially in diabetic cancer patients.^{20,21}

Numerous limitations apply to tablet dosage forms, including poor bioavailability, low local drug concentration, gastrointestinal time fluctuation, dose dumping, and individual variability.²² Dosage reduction and dose frequency reduction are two of the most important purposes of formulation development.²³ If a patient needs to take multiple medications, this causes patient noncompliance and termination of therapy. To overcome the limitations of the most frequently used metformin traditional dosage forms, particulate drug delivery systems, such as microparticles and nanoparticles, can be used.

Metformin has also drawn attention for the treatment of tumors and cancer diseases linked to hyperinsulinemia, particularly breast and colon cancers.²⁴ Cell culture studies have shown that metformin inhibits the proliferation of several cancer cell types, including prostate, breast, endometrial, ovarian, colon, and glioma cells.^{12,25} Studies have shown that patients with diabetes receiving metformin as an antidiabetic medication have varying rates of survival, with suppression of cancer risk factors and cancer-related death.^{12,26} The unique properties of nanoparticles, such as their small size, high surface-area-to-volume ratio, and potential for functionalization with specific targeting moieties, make them ideal for cancer therapy.²⁷ Nanotechnology based metformin has recently gained interest as a potential anticancer agent due to its ability to inhibit cancer cell proliferation, induce apoptosis, and inhibit angiogenesis.²⁸

The primary purpose of this study was to formulate metformin hydrochloride microspheres and nanoparticles to enhance their bioavailability and minimize toxicity and side effects by retarding their action and optimizing their drug-release characteristics. These formulations may have a potential role in reducing hyperglycemic conditions and have anticancer activity.

Materials and Methods

Materials

Trimethylammonium ethyl methacrylate (Eudragit) RSPO (Evonik, Germany), liquid paraffin (Merck, Germany), acetone (Merck, Germany), polyvinyl alcohol (Merck, Germany), n-hexane (Merck, Germany), Span 80 (Loba Chemie, India), methanol (Merck, Germany), hydrochloric acid (Merck, Germany), monobasic sodium phosphate, dibasic sodium phosphate, and sodium hydroxide pellets were purchased from Loba Chemie, India. All other reagents and chemicals used were of analytical grade.

Preparation of Metformin HCl Loaded Microspheres and Nanoparticles

Using the same polymer (Eudragit RSPO) and active pharmaceutical ingredient (API) and their different statistical ratios, four batches of microspheres (A1, A2, A3 and A4) were prepared using the solvent evaporation method, and four batches of nanoparticles (B1, B2, B3, and B4) were prepared using the nanoprecipitation method (Table 1).

Table 1 Formulations Protocol for Microsphere and Nanoparticles

Batch No	Batch Size	Drug Metformin HCl (g)	Eudragit RSPO (g)	Drug Loading (%)
A1	1 g	0.5	0.5	50%
A2	2 g	1.5	0.5	75%
A3	2 g	0.5	1.5	25%
A4	3 g	1.5	1.5	50%
B1	1 g	0.5	0.5	50%
B2	2 g	1.5	0.5	75%
B3	2 g	0.5	1.5	25%
B4	3 g	1.5	1.5	50%

To prepare the microspheres, weighed amounts of Eudragit RSPO were fully dissolved in 20–25 mL of acetone. Then, a weighed amount of metformin HCl was added and the mixture was agitated using an overhead stirrer. The drug–polymer combination was then gradually added to 100 mL of liquid paraffin that had been emulsified earlier with 1% Span 80, while being stirred at 1500 rpm at room temperature using a mechanical stirrer with a triple-blade propeller. The entire system was stirred. The formulated microspheres were kept uninterrupted for a short period to allow for settling. Subsequently, n-hexane was used to wash the settled microspheres numerous times before being dried naturally at room temperature (approximately 25 °C).²⁹

To prepare the nanoparticles, Eudragit RSPO was weighed and dissolved in acetone. A predetermined quantity of metformin HCl was introduced into the PVA (3% w/v) solution before the organic phase was slowly poured into the PVA solution. The mixture was then emulsified for 30 min at 45 °C using an ultrasonicator (Human Lab Instruments and Co., Korea). Centrifugation at 10,000 rpm for 90 min was used to recover the nanoparticles after evaporation of the organic phase during ultrasonication. The nanoparticles were washed twice with distilled water. The nanoparticles were resuspended in distilled water after the final washing, lyophilized, and freeze-dried overnight. Each batch of nanoparticles was created at least three times.³⁰

Characterization of Metformin-Loaded Microspheres and Nanoparticles

Particle Size and Morphological Studies

A laser diffraction particle size analyzer (Partica) was used to determine the particle size distribution (PSD). The microspheres and nanoparticles were mixed with an appropriate solvent while maintaining the same particle diameter. The sample was placed directly into the module and by using dynamic light scattering (DLS), data were gathered for 60s at 25 °C. The volume size distribution was used to compute the particle size. Each study was performed three times, with 24 scans in each run.³¹

In order to examine the shape and surface topography of the microspheres and nanoparticles, scanning electron microscopy (SEM) was used. The formulations were attached to aluminum SEM sample stabs, which were then covered with double-sided adhesive tape, sealed, and enveloped with gold (200 Å) using an ion sputtering apparatus for 15 min at a low pressure (0.001 Torr).²⁹ Using a scanning electron microscope (Zeiss Sigma VP), the platinum-coated materials were imaged at various magnifications to produce photomicrographs at relevant scales (20 µm for microspheres and 5 µm for nanoparticles). Before testing, the microspheres and nanoparticles were dried thoroughly.

Differential Scanning Calorimetry (DSC) Study

Thermograms were collected using a differential scanning calorimeter (DSC) (TA Instruments-Waters LLC, USA) and Trios v5.1.1 software throughout a temperature range of 30–300 °C for 1 h at a flow rate of 20 mL/min and a heating rate of 10 °C/min to test the compatibility between drug and polymer. A sample of metformin microspheres and nanoparticles was placed in an aluminum pan and sealed before heating under nitrogen flow. An empty aluminum pan was used as the reference.³²

Fourier-Transform Infrared (FTIR) Spectroscopy Study

To demonstrate the chemical integrity and compatibility of the formulations, the IR spectra of the pure drug, optimized microspheres, and nanoparticle formulations were obtained. The compatibility between the medicine and excipient in metformin HCl microspheres and nanoparticles was examined using a Fourier-transform infrared (FTIR)/attenuated total reflection (ATR) analyzer. ATR was used instead of FTIR to manufacture the liquids. Direct placement of the sample in the sample holder was used to perform FTIR on samples A1–A4 and B1–B4. A Shimadzu FT-IR 8400S spectrophotometer was used to capture the FT-IR (ATR) spectra with a resolution of 4 cm^{-1} and twenty scans.³³ The samples for metformin HCl were ground into a powder and triturated well with 250 mg of pure fully desiccated powdered potassium bromide (KBr).²⁹ The combination was then formed into a small disc using a specialized mold and hydraulic press. The blends were collected using a diffuse reflectance sampler, and an FTIR spectrophotometer was employed to scan the $400\text{--}4000\text{ cm}^{-1}$ wavelength range and record the spectra.

Measurement of Metformin HCl in Microspheres and Nanoparticles

The drug content in the microspheres was determined as described by Hasan et al (2013), with a slight modification.²⁹ First, 20 mg of microspheres was mixed with 100 mL of buffer, and a vortex mixer was used to obtain a clear solution. The solution was diluted 100 times by adding phosphate buffer. The absorbance was measured at 233 nm. Standard curve analysis was used to convert the absorbance value into the quantity of entrapment.³⁴ The drug entrapment efficiency (EE %) was calculated using the following equation:

$$\text{Drug loading (DL)} = \frac{\text{Weight of the drug in microspheres}}{\text{Weight of the microspheres}} \times 100\%$$

$$\text{Concentration (Sample)} = \frac{\text{Absorbance of sample}}{\text{Absorbance of standard}} \times \text{Concentration (Standard)}$$

$$\text{Entrapment efficiency (\%)} = \frac{\text{Calculated conc.of drug}}{\text{Theoretical conc.of drug}} \times 100\%$$

Drug Loading in the nanoparticles was measured as described by Cetin et al (2013), with slight modifications.³⁰ First, 10 mg of freeze-dried nanoparticles were dissolved in 5 mL of acetone and mixed thoroughly using a vortex mixer. Fresh phosphate buffer (5 mL, pH 6.8) was added to the mixture, which was then centrifuged at 10,000 rpm for 60 min. The absorbance of the solution was measured at 233 nm wavelength. The encapsulation efficiency (EE%) and drug loading (DL%) were determined for each nanoparticle formulation using the following formulas:

Determination of drug loading,

$$\text{Drug loading (DL)} = \frac{\text{Weight of the drug in nanoparticles}}{\text{Weight of the nanoparticles}} \times 100\%$$

Determination of entrapment efficiency (%),

$$\text{Encapsulation efficiency (\%)} = \frac{\text{Calculated concentration of drug}}{\text{Theoretical concentration of drug}} \times 100\%$$

Dissolution Study of Metformin HCl Loaded Microspheres and Nanoparticles

The USP dissolution rate test equipment type II (Paddle type) was used to investigate the dissolution of the microspheres and nanoparticles. The study was conducted for 12 hours in pH 6.8 phosphate buffer media. The absorbance of the collected samples was measured at 233 nm to estimate the quantity of metformin HCl released from microspheres and nanoparticles ([Supplement 1](#)). There was no evidence that additional substances interfered with drug measurement. Plots of drug release % and time were made for each experiment and carried out three times. The average percentage of release for each batch was computed.^{35,36} Data from in vitro drug release investigations were used to fit several kinetic equations to analyze release kinetics. The Higuchi kinetic, zero-order kinetic, first-order kinetic, and Korsmeyer-Peppas models were employed in the kinetic models.

Modified Non-Everted Sac Technique to Assess the in-vitro Intestinal Permeability

The chicken intestinal sac segment was used to measure drug permeability profiles using the modified non-everted sac method in this investigation, in accordance with Gunjal et al (2016) with some modifications.³⁷ Briefly, a predetermined partial segment of the small intestine was cleaned using distilled water followed by phosphate buffer at pH 6.8. The sac was hanged on the shaft of the USP dissolution apparatus II (Paddle type) containing 900 mL of phosphate buffer (pH 6.8) at 37 ± 0.5 °C temperature and 50 rpm stirring speed to evaluate the drug permeability. Metformin-loaded microspheres (Batch No. A4), and nanoparticles (Batch No. B3) were precisely weighed and an equivalent to 5 mg, 10 mg, and 25 mg metformin HCl, respectively, as the original drug content. Each sample was dissolved in 3 mL of phosphate buffer at a pH of 6.8 and the chicken intestinal sac segment was filled with the prepared perfusion solution. The length and diameter of the permeability section were measured during the computation. At specified intervals (1st, 2nd, 3rd, and 6th hour), 5 mL sample aliquots were removed, and a new release medium was introduced to refill each sample. The amount of drug that penetrated the sac segment into the medium was calculated.^{38,39} The permeability coefficient was estimated using Fick's law for isolated chicken guts.⁴⁰

$$dM/dt = PS \times [C_d - C_r],$$

where dM/dt is the number of moles of solute transported per unit time, P is the permeability coefficient, S is the surface area of the membrane, P is the permeability coefficient, C_d is the concentration of solute in the donor [serosal] phase, and C_r is the concentration of solute in the recipient [mucosal] phase.

Because the volume of the serosal fluid is significantly greater than the volume of the mucosa in this situation, sink conditions prevail, and C_r may be disregarded. Thus, the equation can be expressed as:

$$dM/dt = PS \times C_d$$

Mucosal fluid analysis determines M and C_d , and considering the intestinal sac, a cylinder is used to compute S . M/SC_d may then be plotted against time. The slope of the linear plot, calculated using linear regression, represents the permeability coefficient [P] in cm/s.^{41,42}

Assessment of in-vivo Hypoglycemic Activity on Mice

Thirty Healthy Swiss albino mice (20–30 g) were purchased from the International Center for Diarrhoeal Disease Research, Bangladesh (ICDDRDB). The animals were nurtured with the utmost care in a controlled environment with a standard temperature range of (22 ± 2 °C), humidity range of (40–60%), and a light/dark cycle. All animals were subjected to the same conditions and had access to food and water ad libitum. The mice were randomly divided into four groups: a control group without treatment (NC), a positive control treated with metformin HCl powder (MAPI), and two intervention groups treated with the selected formulation A4 of microspheres (A4MS) and formulation B3 of nanoparticles (B3NP). The therapeutic dosage was used to establish a mouse dose of 100 mg/kg.⁴³

The accustomed animals were fasted for 24-hours with only water before being made hyperglycemic using an oral glucose solution with a concentration of 5 mg/mL.^{37,44} The weight and normal fasting blood glucose levels of mice were assessed and reported as fasting blood glucose (FBG) levels prior to the development of the hyperglycemic state. All animals were returned to their cages and provided unrestricted access to normal food and water. After 30 min of glucose administration, blood sugar levels were measured using a glucometer (Safe-Accu 2 Sugar Check: blood glucose monitoring system), and the initial data were entered into an oral glucose tolerance test (OGTT). Immediately following the collection of OGTT data (time 0) after glucose delivery, each group was treated with the corresponding test solution. The blood glucose levels of the mice were measured using a glucometer. Blood samples were collected from the sliced tail tips of conscious mice, and a glucose test strip was inserted after soaking in blood and analyzed using a glucometer. Blood glucose levels were measured after the first, second, third, and sixth hours of oral administration of the test medications.^{37,44}

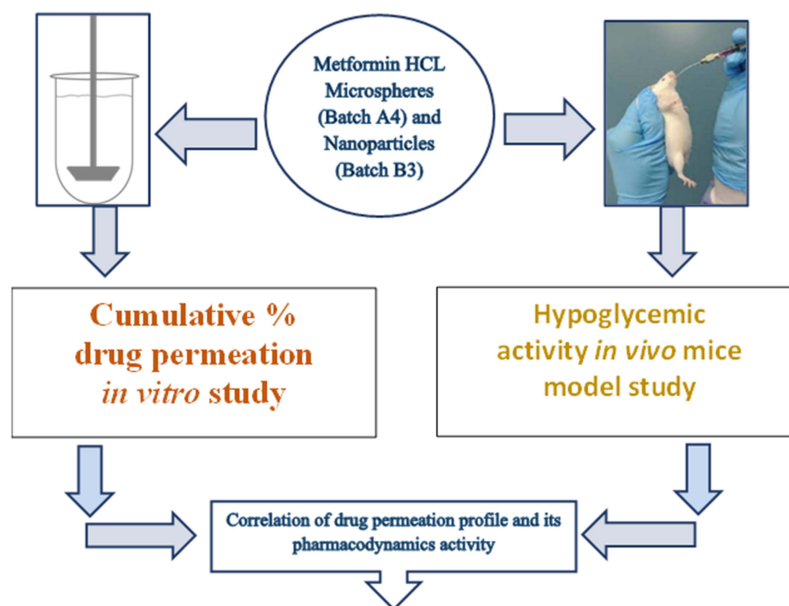


Figure 1 Schematic diagram of drug permeation–pharmacodynamics correlation. Using this schematic diagram, a simple correlation between in vitro pharmacokinetic and in vivo pharmacodynamic study had been tried in this research.

Correlation Between Pharmacokinetic (PK) and Pharmacodynamic (PD) Parameters

In this study, the pharmacodynamic reaction of the drug in the lowering of blood glucose in the mouse model was compared to the in vitro drug penetration profile of the chicken intestinal sac. [Figure 1](#) shows the correlation between drug permeability and percent lowering of blood glucose levels.

Assessment of Ex-Vivo Anticancer Activity of Metformin HCl Nanoparticles

Six samples of nanoparticles were selected to analyze their cytotoxic effects against HeLa cells. Two doses, 500 µg/mL concentration of B2, B3, and B4 formulations, marked as B2A, B3A, and B4A respectively and 250 µg/mL concentration of the same formulations, named B2B, B3B, and B4B, respectively, were used in this assay. Six nanoparticle samples were used for cytotoxicity testing. HeLa, a human cervical cancer cell line, was grown in Dulbecco's modified Eagle's medium (DMEM) supplemented with 1% penicillin-streptomycin (1:1), 0.2% gentamycin, and 10% fetal bovine serum (FBS). On a 96-well plate, cells were planted and incubated at 37 °C with 5% CO₂. Each well received 25 µL of the sample (autoclave) on the following day. After incubation for 48 h, cytotoxicity was assessed using an inverted optical microscope. All samples were analyzed in triplicate.

Statistical Analysis

The DD Solver dissolving software was used to model the release data to determine the drug release mechanism, kinetic models, and release rate. Descriptive statistics, factorial analysis of variance (ANOVA), and repeated-measures ANOVA were applied where necessary. A significance level of 5% was set for hypothesis testing. All data analyses were performed using IBM's SPSS version 25 and R software version 4.2.0.

Results and Discussion

Particle Size and Morphological Studies

The particle size of the solid formulation is a crucial consideration because it has a direct bearing on solubility, which in turn affects the rate and extent of drug release, penetration, and absorption. The mean particle sizes of the microspheres ranged from 2.242 µm to 5.28 µm and nanoparticles from 160.10 nm to 359.90 nm. The mean particle size varied with drug loading percentage. The effects of polymeric concentration on particle size are presented in [Table 2](#).

Table 2 The Effects of Polymeric Concentration, Drug Loading in Total Drug-Polymer Amount on Particle Size

Formulation	Batch no.	Theoretical Drug Loading in Total Amount of Drug Polymer	Particle Size (Mean \pm SD)	Polydispersity Index (PDI)
Microsphere	A1	50% (1g)	5.28 \pm 0.72 μ m	0.40
	A2	75% (2g)	5.53 \pm 0.64 μ m	0.28
	A3	25% (2g)	2.42 \pm 0.93 μ m	0.25
	A4	50% (3g)	4.11 \pm 1.10 μ m	0.15
Nanoparticles	B1	50% (1g)	160.10 \pm 19.07 nm	0.10
	B2	75% (2g)	230.10 \pm 37.31 nm	0.31
	B3	25% (2g)	359.90 \pm 63.08 nm	0.10
	B4	50% (3g)	254.90 \pm 37.63 nm	0.23

Notes: Four batches of microspheres (A1, A2, A3 and A4) and four batches of nanoparticles (B1, B2, B3 and B4).

Both A2 and A3 were prepared in 2 g amounts within fixed 100 mL liquid paraffin. A2, with 75% drug loading, had the highest particle size, whereas A3, with 25% drug loading, had the lowest mean particle size. A1 and A4, both with 50% drug loading, had mean particle sizes ranging from A2 to A3. In the case of nanoparticles, it also describes the same case related to viscosity and particle size. B3 (polymer loading 75%) had the highest mean particle size (359.9 nm) compared with B4 (polymer loading 50%) and B2 (polymer loading 25%). As the polymer concentration increased, the viscosity increased and the particle size decreased.

As the drug concentration increased, the availability of the drug particles for encapsulation increased. The viscosity also increased for a fixed volume of solvent, which led to an increase in the particle size of the microspheres. A3, with a higher drug concentration (75%), showed a particle size greater than that of A2. This was because a lower concentration of the drug was available for the encapsulation of A2. Both A1 and A4, with 50% drug loading, had the same proportion of drug and polymer within a fixed volume of emulsified solvent, although different batch sizes were used. All conditions favored suitable microencapsulation, resulting in a larger particle size than that of A3, but smaller than that of A2. A1 had a larger mean particle size than A4. A1 was prepared in a lower total amount (batch size 1 g), having a larger space area and less viscous environment for encapsulation, resulting in a larger particle size than A4 (batch size 3 g). A previous study reported that drug loading had a direct effect on the particle size of microspheres.²⁹ The size of nanoparticles depends mainly on polymer-derived viscosity rather than on drug loading.³⁰ A higher concentration of the Eudragit polymer in the organic phase causes the organic phase to become more viscous and limits the stirring efficiency, leading to the formation of larger particles.⁴⁵ However, B1, despite having 50% drug loading, had the smallest particle size (160.1 nm). This was due to the low viscosity of the polymer (1 g). These results were in good agreement with those obtained by Valot et al.⁴⁶

The polydispersity indices (PDI) of both microspheres and nanoparticles are displayed in Table 2 and Figure 2a-h. The PDI of formulations A1–A4 and B1–B4 range from 0.154–0.399 and 0.095–0.308, respectively. A4 (PDI 0.154) and B3 (PDI 0.095) had the lowest PDI values, which indicated greater uniformity of particle size compared to other formulations, and all other formulations showed PDI values below 0.4, which indicated uniformity of droplet size. In contrast, higher PDI values for the rest of the formulations indicated the presence of different particle sizes within the same formulation. Aggregation or agglomeration of particles may be the cause of variable particle size. To determine the particle size, polydispersity index (PDI) water was used as a dispersant, with a viscosity of 0.8872 mPa·s and RI of 1.330. Size result quality report for every formulation (except A1) was found to be “Good” which indicates more than

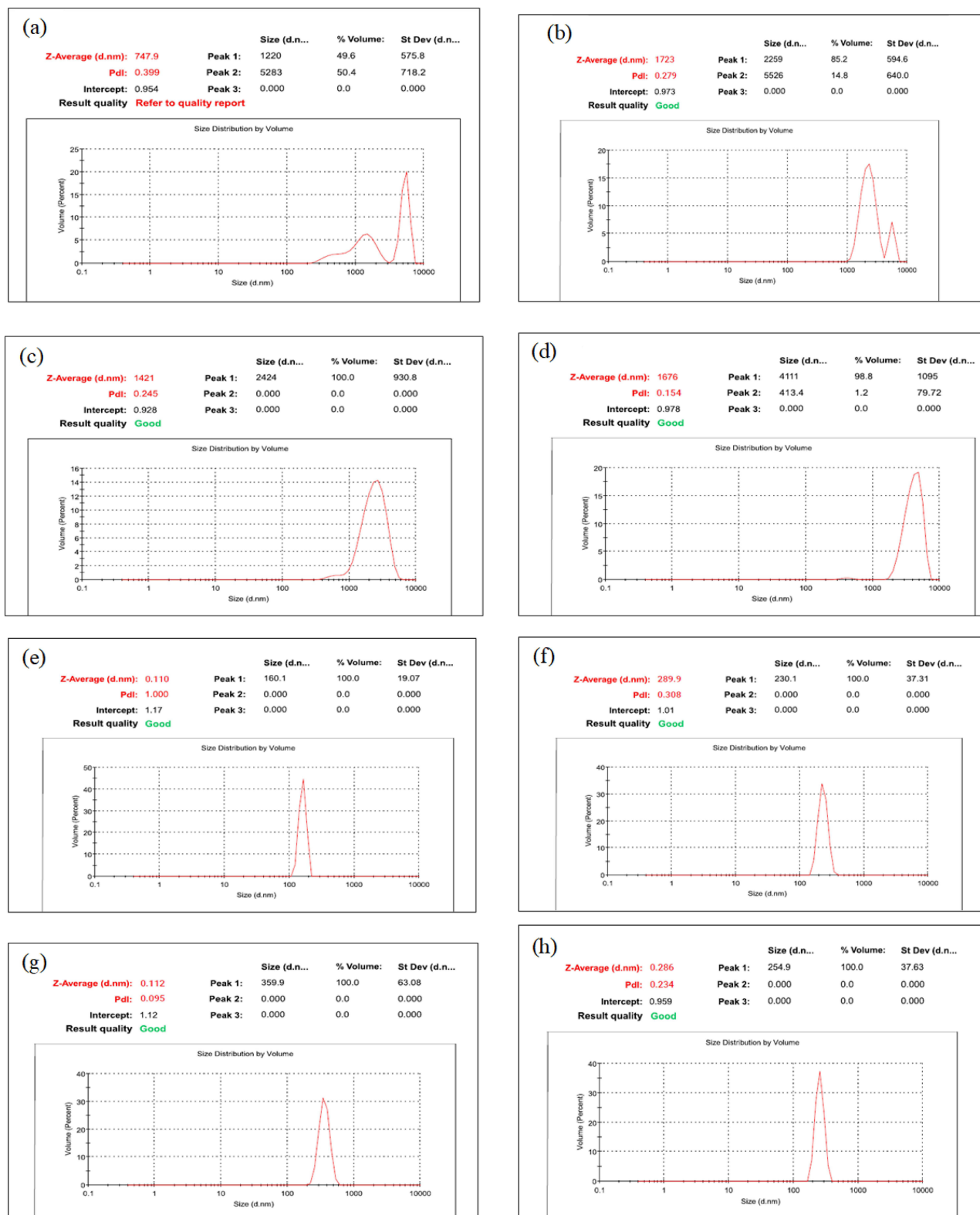


Figure 2 Z-average (nm) value and PDI of Metformin microspheres of batch (a) A1, (b) A2, (c) A3 and (d) A4 and nanoparticles of batch (e) B1, (f) B2, (g) B3 and (h) B4.

80% of the droplets were in the detected size range. The PDI is defined as the ratio of predictable error (standard deviation) to the mean particle size. This indicated the uniformity of the particle size of the formulation. The higher the polydispersity value, the lower is the uniformity of the particle size in the formulation.⁴⁷

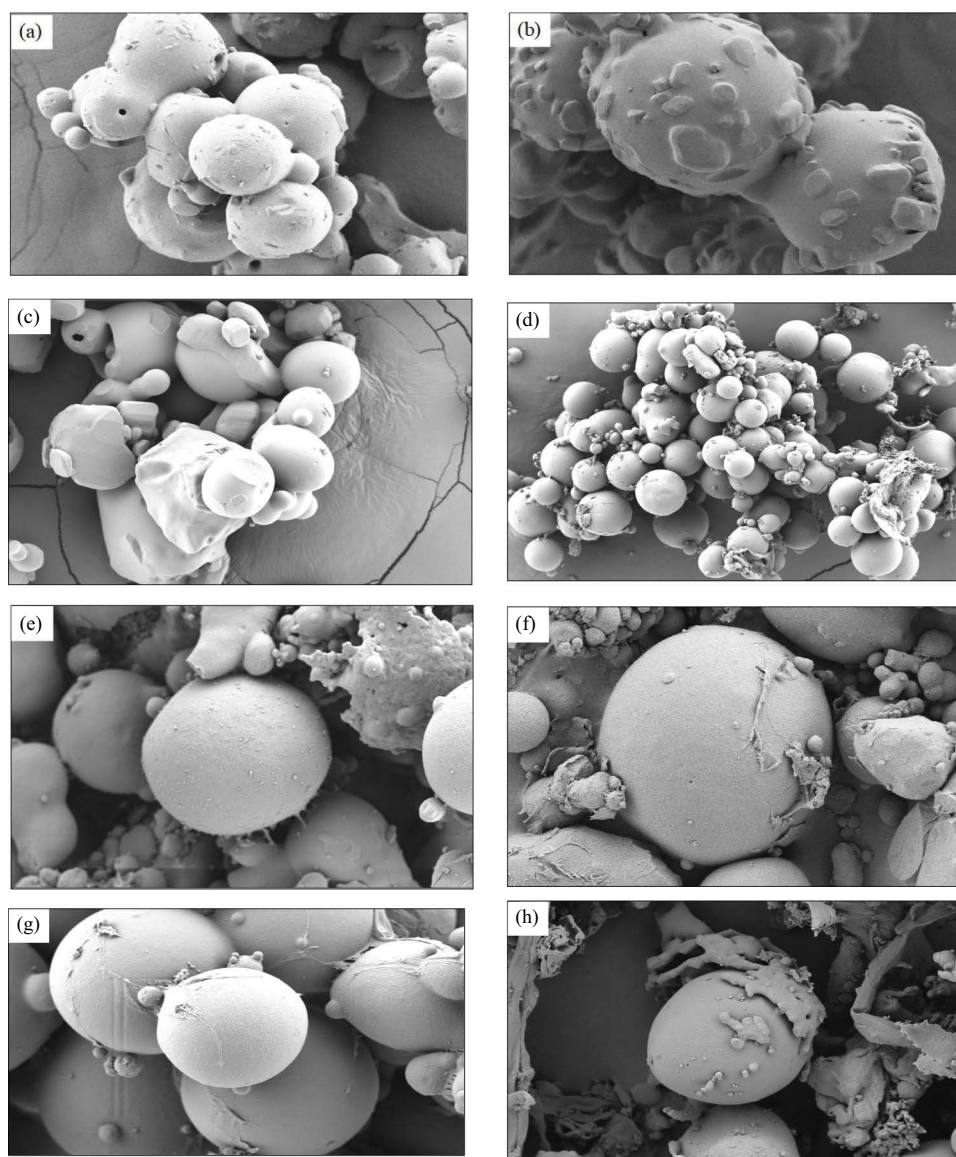


Figure 3 SEM images of metformin microspheres of batch (a) A1, (b) A2, (c) A3 and (d) A4, and nanoparticles of batch (e) B1, (f) B2, (g) B3 and (h) B4.

The SEM images of the metformin HCl-loaded microspheres and nanoparticles were spherical with one or two exceptions with a smooth surface (Figure 3a–h). An uneven surface with adsorbed drug particles was observed for microsphere batch no A2 with 75% drug loading. Again, microsphere batch A3 was nonspherical because of the excess amount of polymer in the formulation. The surfaces of the other batches of microspheres formulated using Eudragit RSPO were relatively smooth, with small amounts of metformin and polymer adsorbed on the surface.²⁹ The excess drug particles adsorbed on the surface were the reason for the initial fast drug release within the first few hours of total dissolution.³⁰ Characterization of the nanoparticle SEM images revealed that Eudragit nanoparticles were more spherical in shape and had a smoother surface than the microspheres. This smoothness contributes to the higher release-retarding capability of nanoparticles compared to that of microspheres.²⁹

Thermal Analysis

Differential scanning calorimetry (DSC) is a quick and accurate method for comprehending polymorphic transitions while examining the compatibility of pharmaceuticals and polymers to learn about potential interactions. DSC measures the energy (heat or electric power) required to maintain the sample and reference at the same comparable temperature as

a function of temperature or time when both are heated at a constant rate. DSC studies were performed on the following samples: pure metformin HCl active pharmaceutical ingredient (API), metformin HCl microspheres of batches A1–A4, and metformin HCl nanoparticles of batches B1–B4.

The DSC curve of pure metformin HCl exhibited an initially flat profile, followed by a single sharp endothermic peak at 230.35 °C representing the melting of the substance in the range 216–230 °C (Tonset = 228.68 °C, Tpeak = 230.35 °C, and $\Delta H_{\text{fusion}} = 429.91$ J/g), which corresponds to pure anhydrous crystalline metformin HCl (Figure S1).^{48,49} No substantial changes were found in the melting points of the microspheres and nanoparticles, in contrast to pure metformin HCl. The endothermic peaks of microspheres A1, A2, A3 and A4 were observed at 226.68 °C, 229.74 °C, 229.16 °C and 226.85 °C, respectively whereas peaks of nanoparticles showed a slight shift from the melting point of the pure peak within the range of 211.02 °C to 220.38 °C, respectively (Figures 4a,b and S2, S3). Moreover, the nanoparticles produced less sharp and shorter melting peaks than the microspheres did.

The presence of melting peaks for metformin implies that there are no interactions occurring in the solid state, which makes it possible to evaluate the compatibility of the drug with polymers in all formulations that were investigated.⁵⁰ As no drastic shifts were observed in the melting points of the microspheres and nanoparticles in contrast to pure metformin HCl, this implied that there was minimal interaction between the drug and polymer.²⁹ In other words, the drugs and polymers were compatible.

Compatibility Study

FTIR evaluation was also carried out for the following samples: pure metformin HCl powder, batches A1–A4 of metformin HCl microspheres and batches B1–B4 of metformin HCl nanoparticles. A study was conducted in which a methodical approach was adopted to investigate metformin HCl using FTIR spectral measurements.⁵¹ Many peaks of pure metformin HCl are visible in these spectra (Table 3 and Figure 5a). The most prominent peaks were primary amine N-H stretching at 3368.23 cm^{-1} , bending at 1621.05 cm^{-1} , imino compound N-H stretching at 3293.51 cm^{-1} , bending at 1559.80 cm^{-1} , secondary amine N-H stretching at 3148.15 cm^{-1} , and bending at 1448.30 cm^{-1} . The spectra of the microspheres prepared using the Eudragit RSPO are shown in Figures 5b and S4. Secondary amine N-H bending and stretching were also observed in the spectra. N-H stretching of the imino compound and N-H bending of the primary amine are also present, but most importantly, N-H bending of the imino compound at approximately 1559.80 cm^{-1} and N-H stretching of the primary amine are present at approximately 3368.23 cm^{-1} , which are reliable signs of the presence of these two groups.²⁹ Batches of nanoparticles (B1–B4) prepared using the same Eudragit RSPO with the same formulation ratio also represent the spectra (Figures 5c and S5). N-H stretching of primary amines, secondary amines, and imino compounds are present in all (except B1), but shifted toward a smaller wavenumber (right) for the latter two, and toward a greater wavenumber (left) for the first one along the X-axis. The N-H bending of the primary and secondary

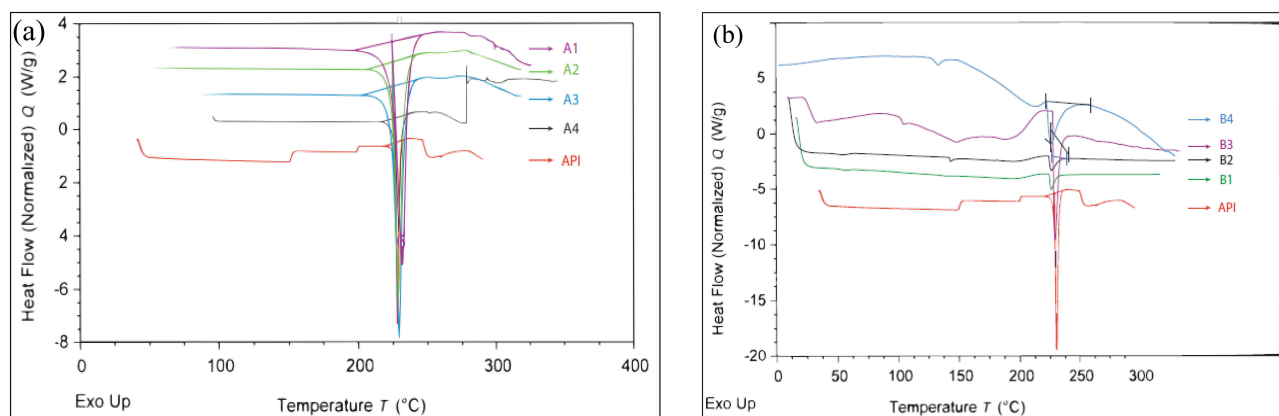


Figure 4 DSC thermogram of all batches of Metformin HCl loaded microspheres (a) and nanoparticles (b) in relation to pure Metformin HCl corresponding to the solid red line in both images. (a) Four batches of microspheres (A1, A2, A3 and A4 designated by solid purple, green, blue and black line respectively) and (b) four batches of nanoparticles (B1, B2, B3 and B4 designated by solid green, black, purple and blue line respectively).

Table 3 FTIR Vibrational Band Assignment of Pure Metformin HCl API

Compound	Tentative Assignment	Frequency (cm ⁻¹)
Metformin HCl	Primary N-H stretching	3372 (sm)
	Asymmetric N-H stretching	3300 (m)
	Symmetric N-H stretching	3176 (m)
	(CH ₃) ₂ N absorption	2619 (vw) - 2816 (w)
	Primary N-H deformation	1583 (s)- 1626 (s)
	Asymmetric N-H deformation	1566 (s)
	Symmetric N-H deformation	1475 (sm)
	N-H deformation	1417 (m)- 1455 (m)
	C-N stretching	1033 (w)-1170(w)
	C-N-C deformation	418-580
	C-H out of plane bending	633 (m)
	N-H out of plane bending	936 (mw)
	NH ₂ rocking	800 (w)
	N-H wagging	736 (mw)

amines showed peaks at approximately 1621.05 cm⁻¹ and 1448.30 cm⁻¹, respectively, without any shift. Both N-H stretching and bending of the imino compound were absent in B1, which can be attributed to any reaction within the formulation. These are legitimate indicators of the presence of these three groups, which indicate limited interaction between the drug and polymer. Therefore, it appears that metformin HCl and Eudragit RSPO are minimally antagonistic to one another, and that there is minimal interaction between metformin HCl and Eudragit RSPO; in other words, they are compatible.²⁹

Drug Content Measurements

Drug loading directly influences the effectiveness of microsphere entrapment. In the case of microspheres, the entrapment efficiency (EE) increased with drug loading, A4 having the highest EE (85.19%), also had the greatest practical drug-loading capacity (42.6% of 50%) (Table 4). In contrast, batch B3 had the highest encapsulation efficiency and highest practical drug loading (Table 4). Studies have reported that drug loading in a particulate system is dependent on a variety of factors, such as the molecular weight (MW), polymer class, and viscosity of the employed organic phase.^{45,52} In general, a higher MW is responsible for achieving high drug loading.⁵³ In contrast, various variables, including interactions between water and solvents, polymers and solvents, polymers and polymers, surfactant concentration, and surfactant type, affect the creation of nanoparticles, yield of nanoparticles, and size of particles. The slightly variable encapsulation efficiency (oppositely affected by drug loading, later supported by statistical analysis) values obtained for metformin HCl-Eudragit[®] RSPO microspheres and nanoparticles could be attributed to the different viscosities of the polymeric phase. A reliable distribution of the medication in the matrix can be obtained by employing an organic phase with higher viscosity.³⁰ In contrast, lowering the viscosity of the organic phase enables the drug to dissolve in the surrounding aqueous medium and come closer to the phase surface during particle formation, resulting in reduced drug content.⁴⁵

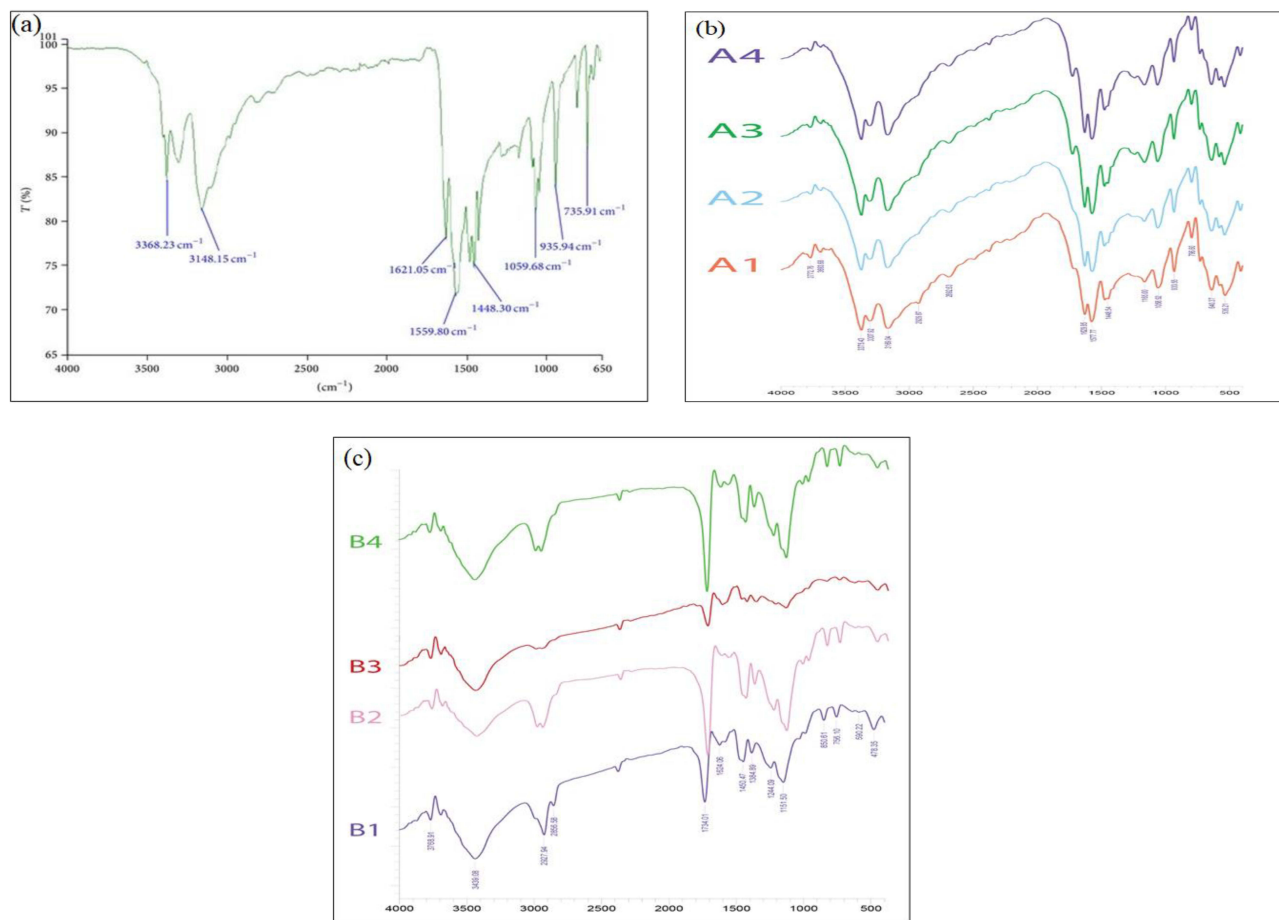


Figure 5 FTIR spectrum of pure metformin HCl powder corresponding to the solid green line (a), all batches metformin HCl loaded microspheres (b) and nanoparticles (c). Four batches of microspheres (A1, A2, A3 and A4 designated by solid Orange, blue, green and purple line respectively) and four batches of nanoparticles (B1, B2, B3 and B4 designated by solid purple, pink, red and green line respectively).

Effect of Drug Loading and Entrapment Ratio on Release Pattern

In vitro drug release study was carried out in Sodium Phosphate buffer at pH 6.8 shown in the [Figures 6a-h](#), [S6](#) and [Table S1-S4](#). Formulation A4 of microspheres and B3 of nanoparticles were showed maximum controlled release effect. Formulation A4 of

Table 4 Calculation of Drug Loading for Metformin HCl Microspheres and Nanoparticles

Batches	Theoretical Drug Loading	Practical Drug Loading	Drug Entrapment Efficiency (EE%)
A1	50%	20.45%	40.94%
A2	75%	50.1%	66.78%
A3	25%	11.48%	45.9%
A4	50%	42.595%	85.19%
B1	50%	20.9%	41.8%
B2	75%	25.11%	33.48%
B3	25%	16.86%	67.43%
B4	50%	22.07%	44.14%

Notes: Four batches of microspheres (A1, A2, A3 and A4) and four batches of nanoparticles (B1, B2, B3 and B4).

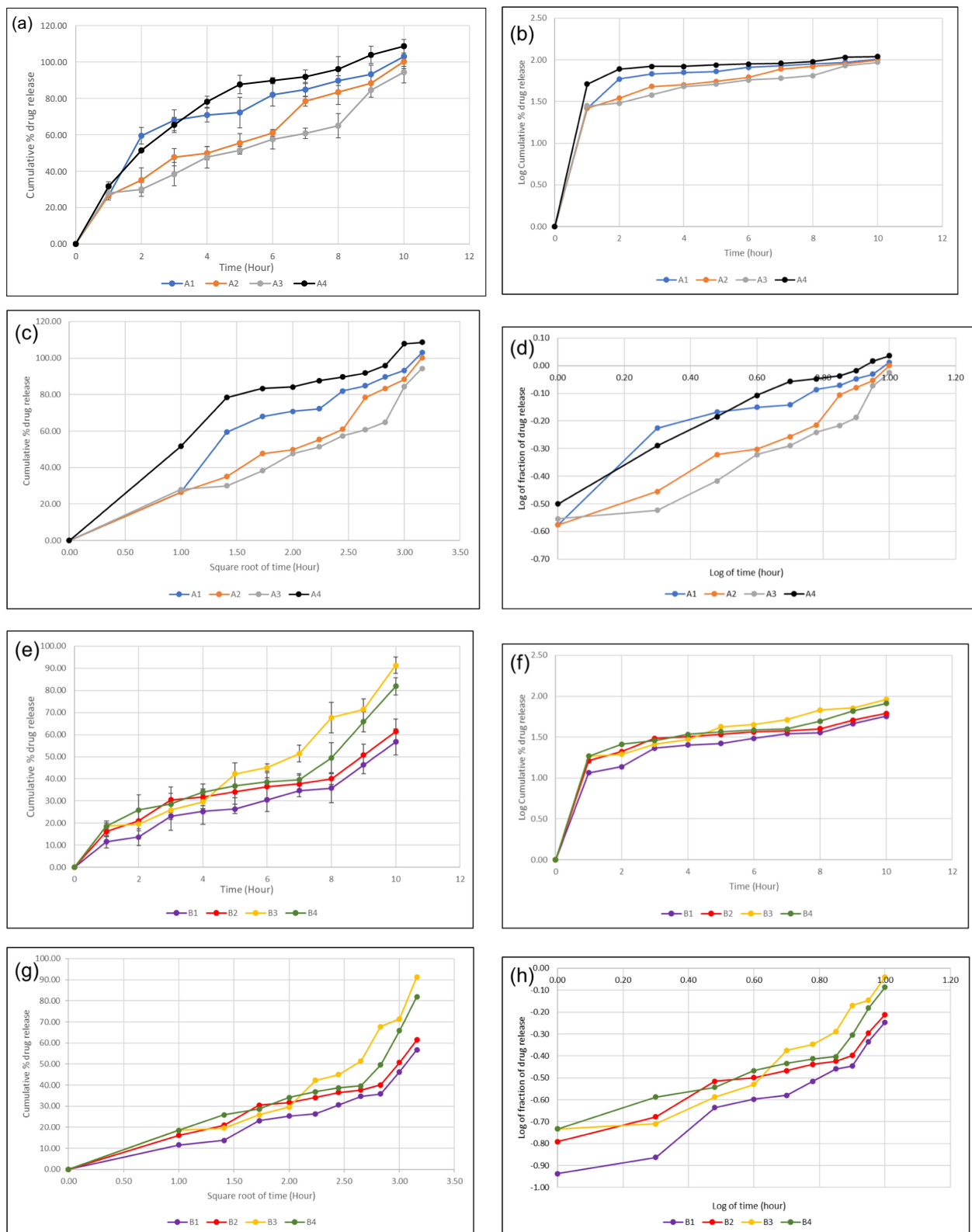


Figure 6 Comparison of cumulative % release in pH 6.8 phosphate buffer of metformin HCl from microspheres and nanoparticles prepared by emulsion solvent evaporation and nanoprecipitation technique respectively, where four formulations of metformin HCl loaded microspheres and nanoparticles indicated to (a and e) for zero order release profile, (b and f) for first order release profile, (c and g) for the Higuchi model and (d and h) for the Korsmeyer–Peppas model respectively. For all microsphere drug release figures (a-d), solid blue, Orange, ash and black line indicates microsphere batch A1, A2, A3 and A4 respectively whereas for all nanoparticles drug release figures (e-h), solid purple, red, yellow and green line indicates nanoparticle batch B1, B2, B3 and B4 respectively.

microspheres was released 103.88% at 9 h, whereas, other formulations of microspheres were taken to release completely around 10 to 11 h. On top of that 91.37% drugs released from formulation B3 of nanoparticles at 10 h, whereas, 56.75%, 61.44%, and 81.94% drugs were from B1, B2 and B4 batch of nanoparticles respectively at the same time (Table S1). Successive fractional dissolution time of microspheres (A1, A2, A3 and A4) and nanoparticles (B1, B2, B3 and B4) has also showed similar results, where A4 of microspheres and B3 of nanoparticles have lower fractional dissolution time compared to others formulations (Table S5).

The drug release outcomes of all formulations of microspheres and nanoparticles were further investigated using kinetic models, including the zero-order, first-order, Higuchi, and Korsmeyer-Peppas models. These different experimental conditions were characterized using the dissolution data. The release rate constants for the microsphere formulations (A1–A4) and nanoparticle formulations (B1–B4) were computed from the slopes of the relevant plots, and the regression coefficient (R²) was established. The release rate constants, regression coefficients (R²), and n values for all formulations of microspheres and nanoparticles, obtained using various kinetic equations, are shown in Tables 5 and 6.

A zero-order plot is used to explain various types of modified release pharmaceutical dosage forms, such as some transdermal systems, matrix tablets with low-solubility medicines, coated forms, and osmotic systems.^{54,55} The application of the first-order plot model in drug dissolution studies was first proposed by Gibaldi and Feldman (1967) and later

Table 5 Summary of Mathematical Kinetics Test of Prepared Formulations

Basic Buffer		Microspheres				Nanoparticles			
		A1	A2	A3	A4	B1	B2	B3	B4
Zero order	K0	11.581	10.300	9.441	12.807	5.292	6.029	8.293	7.256
	R ²	0.6034	0.9018	0.9143	0.0956	0.9278	0.8130	0.9618	0.8699
First order	K1	0.332	0.210	0.172	0.632	0.068	0.082	0.124	0.104
	R ²	0.9571	0.9418	0.9026	0.9388	0.9344	0.8787	0.8986	0.8530
Higuchi	Kh	32.967	28.689	26.145	37.071	13.936	16.130	21.554	19.115
	R ²	0.9624	0.9617	0.9161	0.8380	0.8892	0.9292	0.8353	0.8340
Korsmeyer-Peppas	Kkp	37.979	21.356	16.835	58.283	8.009	13.941	7.978	10.897
	R ²	0.9686	0.9824	0.9511	0.9742	0.9417	0.9283	0.9577	0.9135
	n	0.427	0.650	0.723	0.264	0.793	0.578	1.019	0.797

Table 6 Best Fitted Models for Optimized Formulations

Formulations	Best Fitted Model	n value	Release Mechanism
A1	Korsmeyer-Peppas	0.427	Fickian (case I) diffusion
A2	Korsmeyer-Peppas	0.650	Anomalous / non – Fickian transport
A3	Korsmeyer-Peppas	0.723	Anomalous / non – Fickian transport
A4	Korsmeyer-Peppas	0.264	Fickian (case I) diffusion
B1	Korsmeyer-Peppas	0.793	Anomalous / non – Fickian transport
B2	Korsmeyer-Peppas	0.578	Anomalous / non – Fickian transport
B3	Korsmeyer-Peppas	1.019	Super case II transport
B4	Korsmeyer-Peppas	0.797	Anomalous / non – Fickian transport

by Wagner (1969), which is also used to describe the absorption and elimination of drugs, although it is difficult to conceptualize this mechanism on a theoretical basis.^{56,57} For systems exhibiting case II transport, the dominant mechanism for drug transport is due to polymer matrix relaxation. The diffusional exponent of B specimens indicates non-Fickian/ anomalous type of release mechanism, meaning that drug release couples Fickian diffusion with polymer matrix relaxation - so-called anomalous diffusion -and may indicate that drug release is controlled by more than one process. This together with polymer erosion causes the rapid release after 6 hours.⁵⁸ In 1961, Higuchi proposed the Higuchi plot, which was the first mathematical model to represent drug release from a matrix system.⁵⁹ This model is based on a unique collection of presumptions, including the following: (1) initial drug concentration in the matrix is significantly higher than drug solubility; (2) drug diffusion occurs only in one dimension (edge effect should be avoided); (3) drug particles are much smaller than system thickness; (4) matrix swelling and dissolution are negligible; (5) drug diffusivity is constant; and (6) perfect sink conditions are always attained in the release environment. According to Higuchi, drug release is a diffusion process that depends on the square root of time and is based on Fick's rule. Data were acquired and time was plotted against the square root of the cumulative percentage of drug release.^{60–62} The Korsmeyer–Peppas plot was applied to obtain the drug release pattern using an equation for a polymeric system; the value of “n” was utilized to characterize distinct releases for matrices that are spherical in shape.⁶³

Metformin HCl demonstrated a non-Fickian release from the majority of microsphere and nanoparticle formulations and was found to adhere to the Korsmeyer–Peppas release model. All available evidence points to the controlled release of metformin from microspheres and nanoparticles, which is advantageous for prolonging therapeutic effects as well as for enhancing patient compliance, which is clinically challenging for long-term illnesses such as diabetes.

Evaluation of Intestinal Permeability Study

A comparison of drug permeation over the course of the trial between pure metformin HCl API powder (MAPI) and the two selected formulations, A4 microspheres (A4MS) and B3 nanoparticles (B3NP), is shown in [Figure 7](#) and [Table S6](#). The rate and overall amount of drug that permeated the microspheres significantly increased during the first hour. Nanoparticles coincided with pure drugs, with a small increase in the total drug permeation. The drug permeation profile

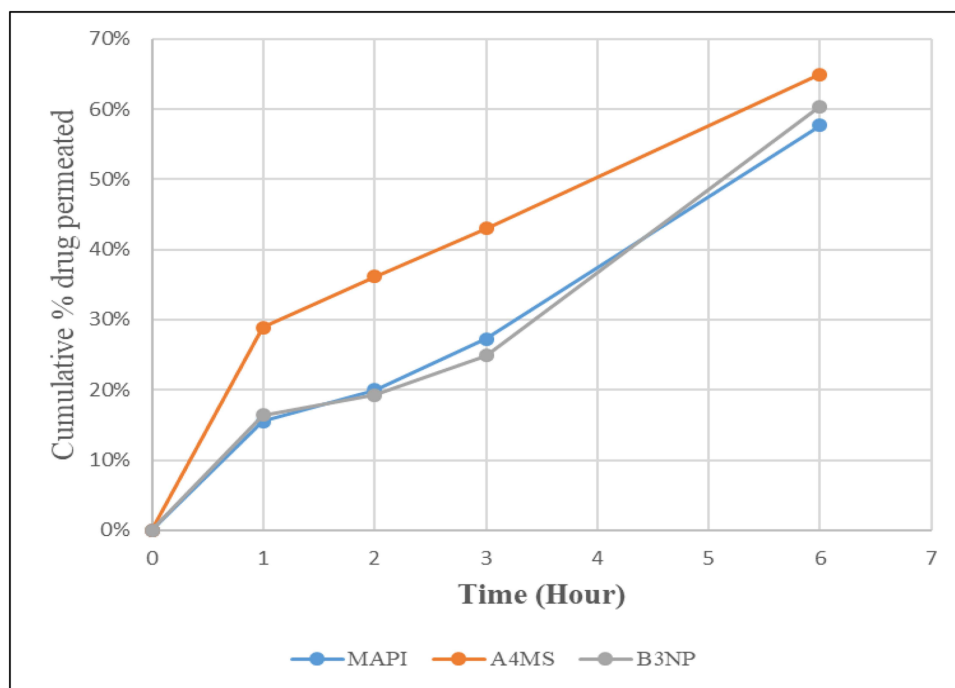


Figure 7 Permeability profiles of metformin HCl API powder (MAPI) indicated by solid red line, selected formulation A4 of microspheres (A4MS) indicated by solid blue line and B3 of nanoparticles (B3NP) indicated by solid green line (n = 3).

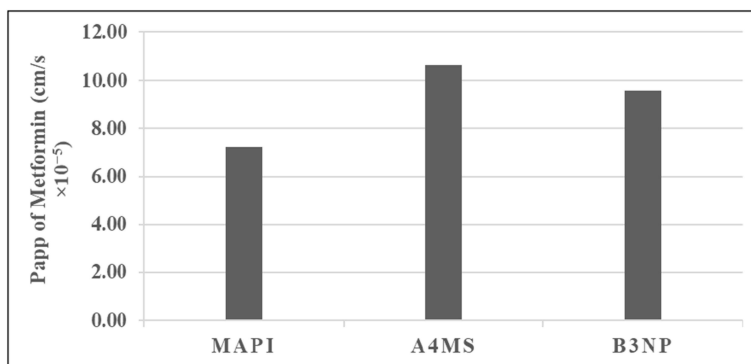


Figure 8 The apparent permeability, Papp (cm/s × 10⁻⁵) of metformin (mucosal -to- serosal) from metformin HCl API powder (MAPI), selected formulation A4 of microspheres (A4MS) and B3 of nanoparticles (B3NP) (n = 3).

increased by 12.62% for the microspheres and 4.68% for the nanoparticles compared to that of the pure drug. It is clear from the table that the values of the regression coefficient, each time, are high enough to take the data's proper fitting into consideration (Figure 8 and Table S7). The lack of lag time may have contributed to the intercept results because of the high-water solubility of the drug. The intercept number demonstrates the rapid saturation of the paracellular pathway in the intestinal wall tissues prior to the drug delivery.³⁹ This result is supported by the fact that the paracellular pathway accounts for 90% of metformin HCl absorption.⁶⁴⁻⁶⁶ All drug penetration parameters increased because of the creation of polymeric microspheres and nanoparticles of metformin. This can be attributed to the role of polymeric encapsulation of the pure drug and an increase in lipid solubility, which in turn results in the enhancement of metformin absorption via the transcellular pathway along with the common paracellular pathway.⁶⁵ The transfer rate of metformin-HCl from the mucosal to the serosal area, in terms of apparent permeability, was higher in microspheres and nanoparticles than in the drug alone (Figure 8). The drug's permeation-enhancing action is caused by the formulation of the drug as micro and nanoparticles.⁶⁷ An enhancement compared to the usual permeability of the drug may lead to a reduction in the recommended dosing of the drug, dosing frequency, and consequently its toxicity or harmful effects, which represent a common problem, especially in older patients.³⁹

Assessment of in-vivo Hypoglycemic Activity

The blood sugar level was measured to represent the initial blood sugar level at the beginning or zero time before the administration of drug formulations. Subsequently, the medication was administered and the plasma glucose level was checked over time. The blood glucose levels at the determined time intervals were plotted as a function of time, which clearly indicated the lowering of blood sugar levels throughout the study (Table 7 and Figure S7). The blood sugar levels in the MAPI groups significantly declined ($p < 0.05$) as well as the blood sugar levels in the A4MS and B3NP groups in

Table 7 Effect of Metformin HCl API Powder (MAPI), Selected Formulation A4 of Microspheres (A4MS) and B3 of Nanoparticles (B3NP) on Blood Sugar Level in Mice Model

Groups	FBS (mmol/L)	OGTT (mmol/L)				
		Zero Hour	1st Hour	2nd Hour	3rd Hour	6th Hour
NC	5.02 ± 2.32	7.33 ± 0.40	7.08 ± 0.15	6.83 ± 2.19	4.97 ± 1.28	4.20 ± 0.95
MAPI	4.38 ± 1.56	7.47 ± 0.41	6.72 ± 0.73	6.25 ± 1.71	4.40 ± 1.01	3.62 ± 1.00
A4MS	5.18 ± 1.24	7.58 ± 0.5	4.15 ± 0.98*	3.72 ± 0.89	3.00 ± 0.79	2.18 ± 0.44
B3NP	4.20 ± 2.37	7.55 ± 0.38	4.91 ± 0.47*	4.61 ± 0.57	3.72 ± 0.48	2.87 ± 0.42

Notes: All data are given as mean ± SD for six animals in each group. Statistically significant results are indicated as (*) $p < 0.05$ versus untreated negative control group (NC).

the first hour compared to the NC group, and no significant difference was observed between the NC and MAPI groups, which is attributed to the drug's high solubility and primary absorption route in the microsphere and nanoparticle forms (paracellular pathway).⁶⁴ As shown in Table 7, the extent and maximum amount of blood sugar reduction was remarkable for the microspheres. Formulations of microspheres and nanoparticles outperformed pure drugs, suggesting that drug absorption is more rapid and has a higher intensity. Previous studies have also demonstrated that nanostructures improve oral bioavailability by inducing the uptake of absorptive endocytosis.⁶⁸

Drug Permeation–Pharmacodynamics Correlation

Monitoring blood sugar levels after oral administration of the medication could be employed as a parameter of pharmacodynamic markers to assess how well metformin HCl from the prepared formulations performed *in-vivo* when compared to the pure medication.

We attempted to establish a mathematical straight-line correlation between the *in vitro* drug penetration percentage and its *in-vivo* pharmacodynamic impact (lowering the sugar level) as a point-to-point correlation between these two variables. Figure 9 provides an overview of the findings. The pharmacodynamic profile of the formulations in the mouse model was nearly superimposed on the drug permeation profile (Figure 9). This may be a result of the strong association between the pharmacodynamic effect and drug permeation percentage. Each time, an increase in the drug permeation percentage led to a reduction in the blood glucose levels.

A modified non-everted sac test, which was employed to demonstrate drug permeation enhancement, also showed that the rate of drug absorption was higher than that of pure drug. Increased drug permeability results in enhanced drug bioavailability, which is reflected in the pharmacodynamic activity of the medication, such as lowering of blood sugar levels. An *in vivo* test was used to test this hypothesis. This discovery should result in a drop in the dosage and frequency at which the drug should be taken, ultimately reducing any adverse effects. Metformin HCl is a BCS class III drug that

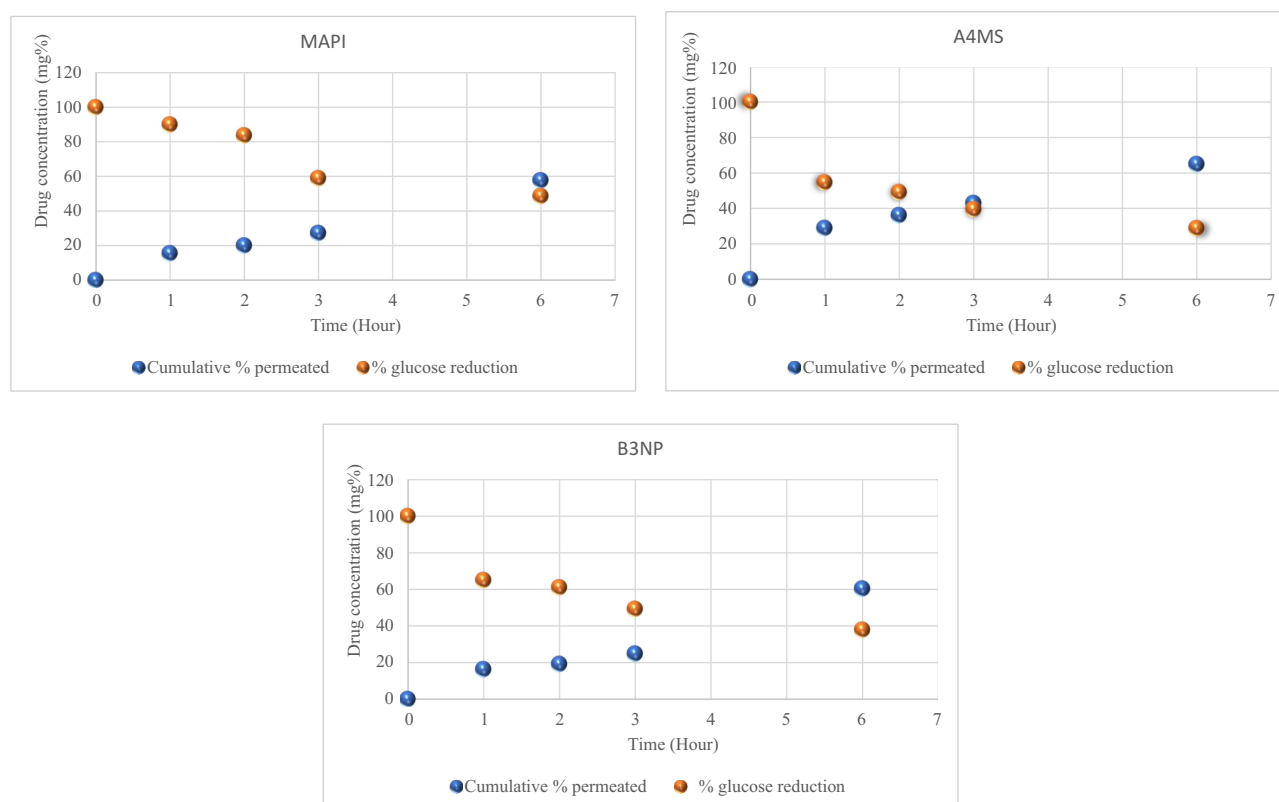


Figure 9 Point to point correlation between the *in-vitro* pharmacokinetic (drug permeation profiles) and its *in-vivo* pharmacodynamic effect (Blood glucose reduction) of metformin HCl API (MAPI), metformin HCl loaded microsphere (A4MS) and nanoparticles (B3NP) whereas, Cumulative % drug permeation is indicated by blue points and reduction of Blood glucose concentration is indicated by Orange points.

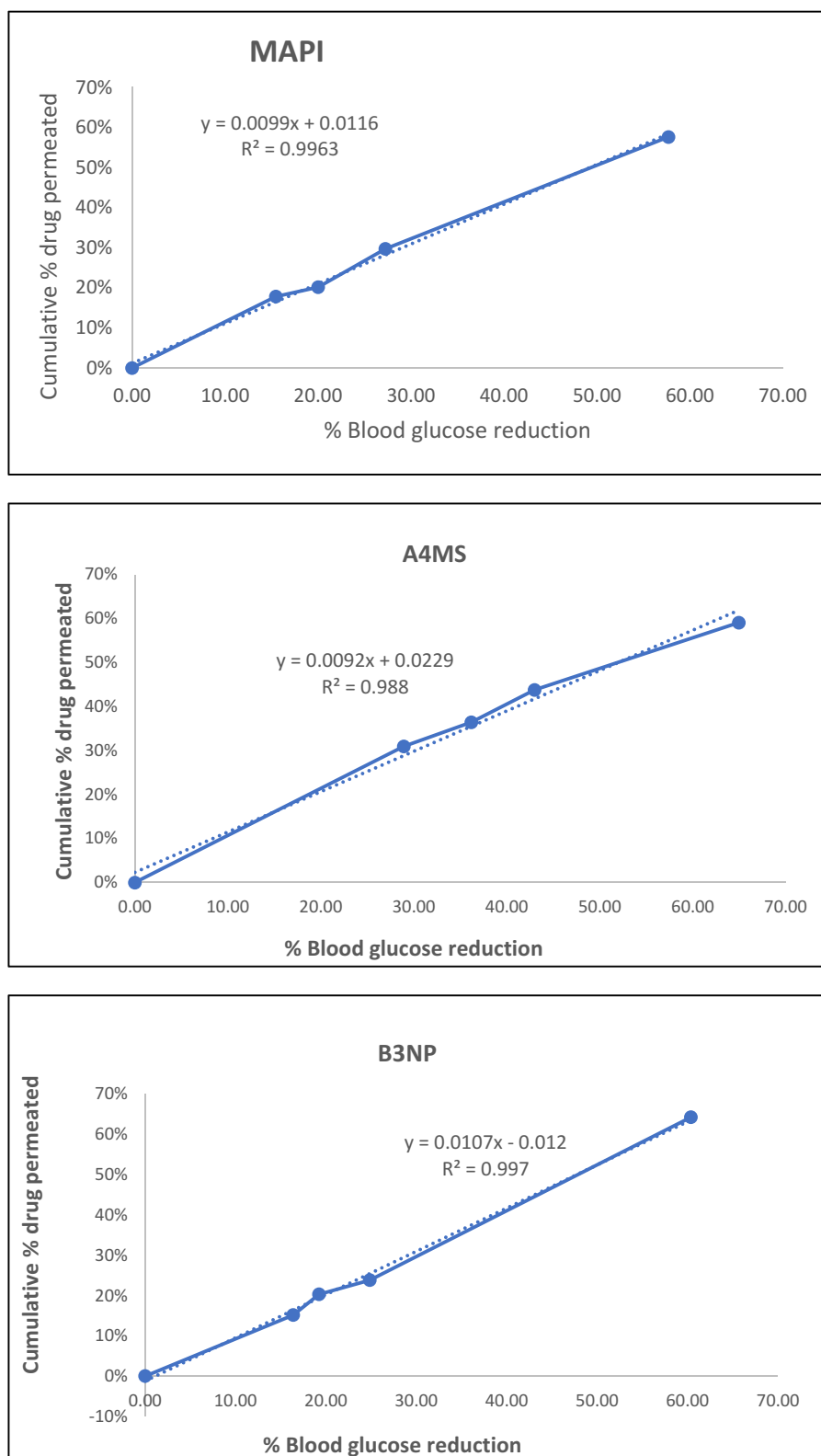


Figure 10 Correlation of the pharmacokinetic (drug permeation profiles) and its pharmacodynamic (hypoglycemic activity) effect: metformin HCl API (MAPI), metformin HCl loaded microspheres (A4MS) and nanoparticles (B3NP).

has permeation problems. Metformin HCl has bioavailability of 40–60%.³⁹ A revised non-everted sac investigation revealed progression of total drug permeation from 57.69% in the MAPI group to 64.97% and 60.39% in the A4MS and B3NP groups, respectively, over 6 h. Similarly, a study on pharmacodynamics indicated that, over the course of six hours, the overall blood glucose reduction percentage improved from 51.41% for MAPI to 71.21% and 62.03% for A4MS and B3NP, respectively. Improvements in the pharmacodynamics of blood sugar level reduction at the same time were 19.8% and 10.62% for microspheres and nanoparticles, respectively, compared to the pure drug in powder form.

These results indicate that metformin-loaded microspheres and nanoparticles have good antidiabetic activities.⁶⁹ Plasma proteins only weakly bind to metformin. It does not undergo hepatic metabolism and is eliminated in the urine.⁷⁰ They primarily enter the body via the paracellular route.⁷¹ In vitro and in vivo studies have shown that liquid-solid systems, SEDDS, and particulate systems improve the solubility and bioavailability of some hydrophilic drugs.^{64,65} In this study, the preparation of metformin microspheres and nanoparticles with polymers increased the partition coefficient (lipophilicity) and decreased the water solubility of metformin. As a result, drug permeability, bioavailability, and pharmacodynamic effects increased.³⁹ This might result in the study of pharmacokinetics, reduction in the dosage of prescribed medications, and undoubtedly, reduction in adverse effects.

As shown in Figure 10, the value of R2 is sufficiently high to infer a strong connection between the variables. These findings support the use of the redesigned non-everted sac as a strategy to predict the in vitro drug permeation process. To avoid a stationary diffusion layer, the intestinal non-everted sac should be suspended in the dissolution apparatus shaft. The circular movement of the blood was represented by the stirring of the dissolving medium by the device shaft. The creation of a stationary diffusion layer is prevented by the dangling of the non-everted sac at the shaft of the dissolution equipment.³⁹ These investigations proved that there may be a strong link between the results of drug permeation from the revised non-everted sac and the reduction in blood sugar levels, thus improving the pharmacodynamic response of the drug.

Assessment of Anticancer Activity of Metformin HCl Nanoparticles

Table 8 and Figure 11 show the cytotoxic activities of nanoparticles. Nearly 100% of the cancerous HeLa cells were cultured with or without a solvent. However, cells showed poor susceptibility when cultured with nanoparticles. 10–20% of cancerous cells survived at 500 µg/mL concentration of B2, B3, and B4 formulations, marked as B2A, B3A, and B4A,

Table 8 Effect of Metformin HCl Nanoparticles on Cancerous HeLa Cell Line

Samples	Percentage of Survival HeLa Cells
Solvent -	100%
Solvent +	More than 95%
B2A	10%- 20% (Cytotoxic to cancer cells)
B3A	10%- 20% (Cytotoxic to cancer cells)
B4A	10%- 20% (Cytotoxic to cancer cells)
B2B	More than 95% (no anticancer property)
B3B	10%- 20% (Cytotoxic to cancer cells)
B4B	20%- 30% (Cytotoxic to cancer cells)

Notes: HeLa cells were cultured with different samples, such as with (Solvent +) or without (Solvent-) solvent, 500µg/mL concentration of B2, B3, and B4 formulations marked as B2A, B3A and B4A respectively and 250µg/mL concentration of B2, B3, and B4 formulations named as B2B, B3B and B4B, respectively of metformin loaded nanoparticles.

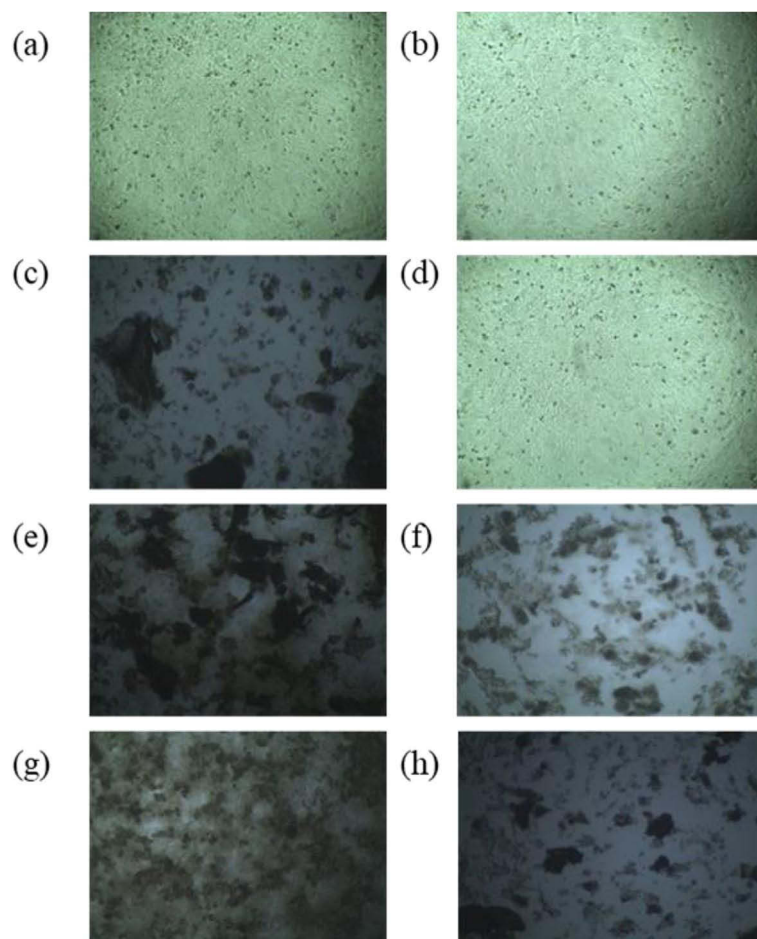


Figure 11 Effect of Metformin HCl Nanoparticles on cancerous HeLa cell line. HeLa cells were cultured with different samples, such as without solvent(a) or with solvent (b), 500 µg/mL concentration of B2, B3, and B4 formulations marked as B2A (c), B3A (e) and B4A (g), respectively and 250 µg/mL concentration of B2, B3, and B4 formulations named as B2B (d), B3B (f) and B4B (h), respectively of metformin loaded nanoparticles.

respectively, confirming their anticancer properties. In addition, a similar result was found in both B3B and B4B at 250 µg/mL concentration groups, similar to the previous three batches. An average of 20% of the cells survived in both groups. However, an opposite trend was observed in the B2B group. The B2B nanoparticles exhibited no cytotoxicity against HeLa cells.

These results are in good agreement with previous findings. When compared to pure metformin, it was discovered that drugs in nanoparticle form were more deadly than API for the growth of pancreatic cancer cells.³ Metformin, a common diabetes medication, is the recommended course of action for the treatment of type II diabetes. Recent reports have asserted that diabetic medications can also shield cancer users. This has sparked much interest in diabetes medication as a potential cancer treatment.⁴⁶ Recent studies have indicated that the treatment of cancers associated with hyperinsulinemia, particularly breast and colon/colorectal cancers, may involve the use of metformin particulate systems as anticancer drugs. In cell culture studies, metformin microparticles, particularly nanoparticles, have been shown to decrease and suppress the proliferation of several cancer cells, including prostate, breast, endometrial, ovarian, colon, and glioma cells, in cell culture studies.^{11,49,72} Another study⁷³ used an ionic gelation approach to create metformin HCl-loaded O-carboxymethyl chitosan nanoparticles for drug delivery to pancreatic cancer cells. Spherical nanoparticles had an average size of 230.50 nm. Metformin HCl and metformin HCl-loaded chitosan nanoparticles displayed stronger harmful effects on pancreatic cancer cells (MiaPaCa-2) than blank nanoparticles, despite the fact that pure metformin and metformin-loaded nanoparticles had no toxic effect on normal cells (L929).

The direct and indirect insulin-dependent activities of metformin have been linked to its anticancer properties. It stops the growth of cancer cells by activating AMPK, Src tyrosine kinase, and mitogen-activated protein kinase (MAPK), repressing mammalian target of rapamycin signaling and protein synthesis, and downregulating EGFR.⁷⁴ In addition, metformin may target cancer-causing cells. The lowering effects of metformin on blood insulin levels may play a significant role in its anticancer action because obesity and elevated insulin levels are major risk factors for various cancer types.⁷² Metformin reduces cancer risk and cancer-related mortality in diabetic patients compared with diabetic patients not treated with metformin.^{11,72} These findings from studies and cytotoxicity testing unequivocally show that metformin HCl nanoparticles have anticancer potential, opening up a novel avenue for the treatment of cancer, particularly in diabetic cancer patients with diabetes.

Conclusion

Metformin HCl-loaded microspheres and nanoparticles were successfully produced in this study, displaying controlled drug release characteristics both in vitro and in vivo as well as anticancer potential. Different ratios (25%, 50%, and 75% drug loading) of metformin HCl and Eudragit RSPO were used to formulate four microspheres and four nanoparticle formulations, which were characterized using PSD, SEM, DSC, and FTIR tests. SEM images illustrated the smooth and spherical nature of all formulations, which are responsible for the drug release-retarding characteristics. The FTIR and DSC results of all formulations showed drug-polymer compatibility. A dissolution study was conducted for 10 hours in pH 6.8 buffer media and drug release from the formulations was primarily controlled by a non-Fickian diffusion process, with some exceptions. The best-fit model for the maximum formulations was Korsmeyer–Peppas. A4 from the microspheres and B3 from the nanoparticles exhibited greater drug release, drug entrapment, and compatibility characteristics, which were attributed to their inclusion in both permeation studies using non-everted intestinal sacs and in animal research using mouse models. Both formulations (A4 and B3) exhibited strong relationships with each other. Almost all nanoparticles were found to be cytotoxic to HeLa cells. The proposed formulations of metformin HCl dramatically reduced hyperglycemic conditions and might also contribute to future cancer studies owing to its anticancer potential. These results open up the possibility of further improving the bioavailability of this antidiabetic drug, which can be used, especially in cancer patients with diabetes.

Ethics Statement

The animal experimental protocol was approved by the Research Ethics Committee of University of Asia Pacific and followed the laboratory animal guideline for ethical review of animal welfare (Ref. no. UAP/REC/2022/110).

Acknowledgments

This research was funded by the Centennial Research Grant, University of Dhaka for the Fiscal Year 2020–21. The authors are thankful to the University of Asia Pacific for providing resources for this research. The authors also thank Ikramul Hasan, Faria Nasrin, Sharmin Akter, and Lamia Alam for technical support.

Disclosure

The authors report no conflicts of interest in this work.

References

1. Kumar CS, Karthikeyan D, Gadela VR. Enhanced effect of Metformin loaded chitosan nanoparticles in L6 Myotubes: in-vitro. *Sch Res J*. 2017;7(7):48–63.
2. Horenstein RB, Shuldiner AR. Genetics of Diabetes. *Rev Endocr Metab Disord*. 2004;5(1):25–36. doi:10.1023/B:REMD.0000016122.84105.75
3. Wild S, Roglic G, Green A, et al. Global Prevalence of Diabetes: estimates for the year 2000 and projections for 2030. *Diabetes Care*. 2004;27(5):1047–1053. doi:10.2337/diacare.27.5.1047
4. Mohan V, Sandeep S, Deepa R, et al. Epidemiology of type 2 diabetes: Indian scenario. *Indian J Med Res*. 2007;125:3.
5. Akiyama S, Katsumata S, Suzuki K, et al. Hypoglycemic and Hypolipidemic Effects of Hesperidin and Cyclodextrin-Clathrated Hesperetin in Goto-Kakizaki Rats with Type 2 Diabetes. *Biosci Biotechnol Biochem*. 2009;73(12):2779–2782. doi:10.1271/bbb.90576

6. Ibrahim HO, Osilesi O, Adebawo OO, et al. In vitro Assessment of the Potential Antioxidant and Antidiabetic Properties of Edible Parts of *Chrysophyllum albidum* Fruit Extracts. *J Food Nutr Res.* 2019;7:105–113.
7. Kearney J, Gnudi L. The Pillars for Renal Disease Treatment in Patients with Type 2 Diabetes. *Pharmaceutics.* 2023;15(5):1343. doi:10.3390/pharmaceutics15051343
8. Viollet B, Guigas B, Garcia NS, et al. Cellular and molecular mechanisms of metformin: an overview. *Clin Sci.* 2011;122(6):253–270. doi:10.1042/CS20110386
9. Grzybowska M, Bober J, Olszewska M. Metformin - mechanisms of action and use for the treatment of type 2 diabetes mellitus. *Postepy Hig Med Dosw.* 2011;65:277–285. doi:10.5604/17322693.941655
10. Balogh DB, Wagner LJ, Fekete A. An Overview of the Cardioprotective Effects of Novel Antidiabetic Classes: focus on Inflammation, Oxidative Stress, and Fibrosis. *Int J Mol Sci.* 2023;24(9):7789. doi:10.3390/ijms24097789
11. Viollet B, Guigas B, Garcia NS, et al. Cellular and molecular mechanisms of metformin: an overview. *Clin Sci.* 2012;122(6):253–270.
12. Dowling RJ, Goodwin PJ, Stambolic V. Understanding the benefit of metformin use in cancer treatment. *BMC Med.* 2011;9(1):33. doi:10.1186/1741-7015-9-33
13. Adikwu MU, Yoshikawa Y, Takada K. Bioadhesive Delivery of Metformin Using Prosopis Gum with Antidiabetic Potential. *Biol Pharm Bull.* 2003;26(5):662–666. doi:10.1248/bpb.26.662
14. Boldhane SP, Kuchekar BS. Gastroretentive Drug Delivery of Metformin Hydrochloride: formulation and In Vitro Evaluation Using 32 Full Factorial Design. *Curr Drug Deliv.* 2009;6(5):477–485. doi:10.2174/156720109789941641
15. Murphy C, Pillay V, Choonara YE, et al. Optimization of a Dual Mechanism Gastrofloatable and Gastroadhesive Delivery System for Narrow Absorption Window Drugs. *AAPS Pharm Sci Tech.* 2012;13(1):1–15. doi:10.1208/s12249-011-9711-1
16. Raparla R, Talasila EKM. Design and evaluation of floating drug delivery systems of metformin with natural gums as release retarding polymers. *Int J Adv Pharm.* 2012;1:22.
17. Amorim MJLG, Ferreira JPM. Microparticles for delivering therapeutic peptides and proteins to the lumen of the small intestine. *Eur J Pharm Biopharm.* 2001;52(1):39–44. doi:10.1016/S0939-6411(01)00148-5
18. Gelperina S, Kisich K, Iseman MD, et al. The Potential Advantages of Nanoparticle Drug Delivery Systems in Chemotherapy of Tuberculosis. *Am J Respir Crit Care Med.* 2005;172(12):1487–1490. doi:10.1164/rccm.200504-613PP
19. Gundogdu N, Cetin M. Chitosan-poly (lactide-co-glycolide) (CS-PLGA) nanoparticles containing metformin HCl: preparation and in vitro evaluation. *Pak J Pharm Sci.* 2014;27(6):1923–1929.
20. Alexis F, Pridgen EM, Langer R, et al. Nanoparticle Technologies for Cancer Therapy. *Drug Deliv.* 2010;197:86.
21. Cetin M, Sahin S. Microparticulate and nanoparticulate drug delivery systems for metformin hydrochloride. *Drug Deliv.* 2016;23(8):2796–2805. doi:10.3109/10717544.2015.1089957
22. Wen H, Jung H, Li X. Drug Delivery Approaches in Addressing Clinical Pharmacology-Related Issues: opportunities and Challenges. *AAPS J.* 2015;17(6):1327–1340. doi:10.1208/s12248-015-9814-9
23. Janczura M, Sip S, Cielecka-Piontek J. The Development of Innovative Dosage Forms of the Fixed-Dose Combination of Active Pharmaceutical Ingredients. *Pharmaceutics.* 2022;14(4):834. doi:10.3390/pharmaceutics14040834
24. Yu H, Zhong X, Gao P, et al. The Potential Effect of Metformin on Cancer: an Umbrella Review. *Front Endocrinol.* 2019;10:617. doi:10.3389/fendo.2019.00617
25. Kourelis TV, Siegel RD. Metformin and cancer: new applications for an old drug. *Med Oncol.* 2012;29(2):1314–1327. doi:10.1007/s12032-011-9846-7
26. Ganjali M, Ganjali H. Anticancer Effect of Metformin, an antidiabetic drug, on breast Cancer Cells. *J Nov Appl Sci.* 2013;2:796–801.
27. Xu X, Ho W, Zhang X, et al. Cancer nanomedicine: from targeted delivery to combination therapy. *Trends Mol Med.* 2015;21(4):223–232. doi:10.1016/j.molmed.2015.01.001
28. Aljofan M, Riethmacher D. Anticancer activity of metformin: a systematic review of the literature. *Future Sci OA.* 2019;5(8):410. doi:10.2144/fsoa-2019-0053
29. Hasan I, Paul S, Akhter S, et al. Evaluation and Optimization of Influence of Permeability Property and Concentration of Polymethacrylic Polymers on Microspheres of Metformin HCl. *Dhaka Univ J Pharm Sci.* 2013;12:2.
30. Cetin M, Atila A, Sahin S, et al. Preparation and characterization of metformin hydrochloride loaded-Eudragit® RSPO and Eudragit® RSPO/PLGA nanoparticles. *Pharm Dev Technol.* 2013;18(3):570–576. doi:10.3109/10837450.2011.604783
31. Deryabin DG, Efremova LV, Vasilchenko AS, et al. A zeta potential value determines the aggregate's size of penta-substituted [60]fullerene derivatives in aqueous suspension whereas positive charge is required for toxicity against bacterial cells. *J Nanobiotechnol.* 2015;13(1):50. doi:10.1186/s12951-015-0112-6
32. Corti G, Cirri M, Maestrelli F, et al. Sustained-release matrix tablets of metformin hydrochloride in combination with triacetyl- β -cyclodextrin. *Eur J Pharm Biopharm.* 2008;68:303–309.
33. Valot P, Baba M, Nedelec JM, et al. Effects of process parameters on the properties of biocompatible Ibuprofen-loaded microcapsules. *Int J Pharm.* 2009;369(1–2):53–63. doi:10.1016/j.ijpharm.2008.10.037
34. Baboota S, Shakeel F, Ahuja A, et al. Design development and evaluation of novel nanoemulsion formulations for transdermal potential of Celecoxib. *Acta Pharm Zagreb Croat.* 2007;57:315–332.
35. Block LC, Schmeling LO, Couto AG, et al. Effect of binders on 500mg metformin hydrochloride tablets produced by wet granulation. *Rev Ciênc Farm Básica E Apl.* 2009;30:2.
36. Wadher KJ, Kakde RB, Umekar MJ. Study on sustained-release metformin hydrochloride from matrix tablet: influence of hydrophilic polymers and in vitro evaluation. *Int J Pharm Investig.* 2011;1(3):157–163. doi:10.4103/2230-973X.85966
37. Veiga A, Oliveira PR, Bernardi LS, et al. Solid-state compatibility studies of a drug without melting point. *J Therm Anal Calorim.* 2018;131(3):3201–3209. doi:10.1007/s10973-017-6756-8
38. Sheela NR, Muthu S, Krishnan SS. FTIR, FT Raman and UV-visible spectroscopic analysis on metformin hydrochloride. *Asian J Chem.* 2010;22:5049.
39. Piao J, Lee JE, Weon KY, et al. Development of novel mucoadhesive pellets of metformin hydrochloride. *Arch Pharm Res.* 2009;32(3):391–397. doi:10.1007/s12272-009-1312-0

40. Sundaramoorthy R, Raju MDD. Self-emulsifying drug delivery system: a review. *WJPPS*. 2012;2:89–107.
41. Freitas MN, Marchetti JM. Nimesulide PLA microspheres as a potential sustained release system for the treatment of inflammatory diseases. *Int J Pharm*. 2005;295(1–2):201–211. doi:10.1016/j.ijpharm.2005.03.003
42. Libo Y, Reza F. Kinetic modeling on drug release from controlled drug delivery system. *J Pharm Sci*. 1996;85(2):170. doi:10.1021/js950250r
43. Gibaldi M, Feldman S. Establishment of sink conditions in dissolution rate determinations. Theoretical considerations and application to nondisintegrating dosage forms. *J Pharm Sci*. 1967;56(10):1238–1242. doi:10.1002/jps.2600561005
44. Dewan I, Islam S, Rana MS. Characterization and Compatibility Studies of Different Rate Retardant Polymer Loaded Microspheres by Solvent Evaporation Technique: in Vitro-In Vivo Study of Vildagliptin as a Model Drug. *J Drug Deliv*. 2015;2015:496807. doi:10.1155/2015/496807
45. Kalam MA, Humayun M, Parvez N, et al. Release Kinetics of Modified Pharmaceutical Dosage Forms: a Review. *Cont J Pharm Sci*. 2007;1:30–35.
46. Desai SJ, Singh P, Simonelli AP, et al. Investigation of factors influencing release of solid drug dispersed in inert matrices II: quantitation of procedures. *J Pharm Sci*. 1966;55(11):1224–1229. doi:10.1002/jps.2600551112
47. Jain A, Jain SK. In vitro release kinetics model fitting of liposomes: an insight. *Chem. Phys. Lipids*. 2016;201:28–40. doi:10.1016/j.chemphyslip.2016.10.005
48. Rivas CJM, Tarhini M, Badri W, et al. Nanoprecipitation process: from encapsulation to drug delivery. *International Journal of Pharmaceutics*. 2017;532(1):66–81. doi:10.1016/j.ijpharm.2017.08.064
49. Korsmeyer RW, Gurny R, Doelker E, et al. Mechanisms of solute release from porous hydrophilic polymers. *Int J Pharm*. 1983;15(1):25–35. doi:10.1016/0378-5173(83)90064-9
50. Mady OY, Al-Shoubki AA, Donia AA. An Industrial Procedure for Pharmacodynamic Improvement of Metformin HCl via Granulation with Its Paracellular Pathway Enhancer Using Factorial Experimental Design. *Drug Des Devel Ther*. 2021;15:4469–4487. doi:10.2147/DDDT.S328262
51. Deli MA. Potential use of tight junction modulators to reversibly open membranous barriers and improve drug delivery. *Biochim Biophys Acta BBA - Biomembr*. 2009;1788:892–910.
52. Dimitrijevic D, Shaw AJ, Florence AT. Effects of Some Non-ionic Surfactants on Transepithelial Permeability in Caco-2 Cells. *J Pharm Pharmacol*. 2000;52:157–162. doi:10.1211/0022357001773805
53. Subramanian N, Sharavanan SP, Chandrasekar P, et al. Lacidipine self-nanoemulsifying drug delivery system for the enhancement of oral bioavailability. *Arch Pharm Res*. 2016;39(4):481–491. doi:10.1007/s12272-015-0657-9
54. Ghasemiyeh P, Mohammadi-Samani S. Potential of Nanoparticles as Permeation Enhancers and Targeted Delivery Options for Skin: advantages and Disadvantages. *Drug Des Devel Ther*. 2020;14:3271–3289. doi:10.2147/DDDT.S264648
55. Park SH, Oh SG, Mun JY, et al. Loading of gold nanoparticles inside the DPPC bilayers of liposome and their effects on membrane fluidities. *Colloids Surf B Biointerfaces*. 2006;48(2):112–118. doi:10.1016/j.colsurfb.2006.01.006
56. Hughes SG. Prescribing for the elderly patient: why do we need to exercise caution? *Br J Clin Pharmacol*. 1998;46(6):531–533. doi:10.1046/j.1365-2125.1998.00842.x
57. Graham GG, Punt J, Arora M, et al. Pharmacokinetic of Metformin. *Clin Pharmacokinet*. 2011;50(2):81–98. doi:10.2165/11534750-000000000-00000
58. Apu AS, Pathan AH, Shrestha D, et al. Investigation of in vitro release kinetics of carbamazepine from Eudragit® RS PO and RL PO matrix tablets. *Trop J Pharm Res*. 2009;8(2):145–152. doi:10.4314/tjpr.v8i2.44523
59. Dahan A, Porat D, Markovic M, et al. Optimized In Silico Modeling of Drug Absorption after Gastric Bypass: the Case of Metformin. *Pharmaceutics*. 2021;13(11):1873. doi:10.3390/pharmaceutics13111873
60. Varde NK, Pack DW. Microspheres for controlled release drug delivery. *Expert Opin Biol Ther*. 2004;4:35–51. doi:10.1517/14712598.4.1.35
61. Yu LX, Amidon GL, Polli JE, et al. Biopharmaceutics classification system: the scientific basis for biowaiver extensions. *Pharma Res*. 2002;19:921–925. doi:10.1023/A:1016473601633
62. Kawabata Y, Wada K, Nakatani M, et al. Formulation design for poorly water-soluble drugs based on biopharmaceutics classification system: basic approaches and practical applications. *Int J Pharm*. 2011;420(1):1–10. doi:10.1016/j.ijpharm.2011.08.032
63. Ritger PL, Peppas NA. A simple equation for description of solute release II. Fickian and anomalous release from swellable devices. *J Control Release*. 1987;5(1):37–42. doi:10.1016/0168-3659(87)90035-6
64. Kendre PN, Chaudhari PD. Effect of polyvinyl caprolactam–polyvinyl acetate–polyethylene glycol graft copolymer on bioadhesion and release rate property of eplerenone pellets. *Drug Dev Ind Pharm*. 2017;43:751–761. doi:10.1080/03639045.2016.1220570
65. Hasan AA, Madkor H, Wageh S. Formulation and evaluation of metformin hydrochloride-loaded niosomes as controlled release drug delivery system. *Drug Deliv*. 2013;20(3–4):120–126. doi:10.3109/10717544.2013.779332
66. Saha AK, Ray SD. Effect of cross-linked biodegradable polymers on sustained release of sodium diclofenac-loaded microspheres. *Braz J Pharm Sci*. 2013;49(4):873–888. doi:10.1590/S1984-82502013000400028
67. Sarkar K, Sadat SMA, Islam MS, et al. Study of Ethyl Cellulose Based Sustained Release Microspheres of Naproxen Sodium. *Dhaka Univ J Pharm Sci*. 2011;10:2.
68. Gunjal A, Walunj M, Aghera H, et al. Hypoglycemic and anti-hyperglycemic activity of Triphalādi granules in mice. *Anc Sci Life*. 2016;35(4):207–211. doi:10.4103/0257-7941.188177
69. Ashwell M, Stone EM, Stolte H, et al. UK Food Standards Agency Workshop Report: an investigation of the relative contributions of diet and sunlight to vitamin D status. *Br J Nutr*. 2010;104(4):603–611. doi:10.1017/S0007114510002138
70. Almoazen H. Chapter 4: dosage forms and drug delivery systems. *APhA Complete Rev Pharm*. 2017.
71. Page DA, Carlson GP. Method for Studying the Permeability of the Rat Intestinal Tract to Carbon Tetrachloride. *Toxicol Methods*. 1991;1(3):188–198. doi:10.3109/15376519109044569
72. Arcidiacono B, Iiritano S, Nocera A, et al. Insulin resistance and cancer risk: an overview of the pathogenetic mechanisms. *Exp Diabetes Res*. 2012;2012:789174. doi:10.1155/2012/789174
73. Pereira ASBF, Lima MLS, Silva-Junior AA, et al. In vitro-in vivo availability of metformin hydrochloride-PLGA nanoparticles in diabetic rats in a periodontal disease experimental model. *Pharm Biol*. 2021;59(1):1574–1582. doi:10.1080/13880209.2021.2002369
74. Kumar K, Pant NC, Ahmad S, et al. Development and evaluation of floating microspheres of curcumin in alloxan-induced diabetic rats. *Trop J Pharm Res*. 2016;15(9):9. doi:10.4314/tjpr.v15i9.1

Drug Design, Development and Therapy

Dovepress

Publish your work in this journal

Drug Design, Development and Therapy is an international, peer-reviewed open-access journal that spans the spectrum of drug design and development through to clinical applications. Clinical outcomes, patient safety, and programs for the development and effective, safe, and sustained use of medicines are a feature of the journal, which has also been accepted for indexing on PubMed Central. The manuscript management system is completely online and includes a very quick and fair peer-review system, which is all easy to use. Visit <http://www.dovepress.com/testimonials.php> to read real quotes from published authors.

Submit your manuscript here: <https://www.dovepress.com/drug-design-development-and-therapy-journal>